

## ARTICLES

# Substrate Trafficking and Dioxygen Activation in Bacterial Multicomponent Monooxygenases

LESLIE J. MURRAY AND STEPHEN J. LIPPARD\*

*Department of Chemistry, Massachusetts Institute of Technology, Cambridge, Massachusetts 02139*

Received December 12, 2006

**ABSTRACT**

Non-heme carboxylate-bridged diiron centers in the hydroxylase components of the bacterial multicomponent monooxygenases process four substrates during catalysis: electrons, protons, dioxygen, and hydrocarbons. Understanding how protein–protein interactions mediate the transport of these substrates to the diiron center to achieve the selective oxidation of the hydrocarbon is a significant challenge. In this Account, we summarize our current knowledge of these processes with a focus on the methane monooxygenase system. We also describe recent results for the toluene/*o*-xylene monooxygenase and phenol hydroxylase systems from *Pseudomonas* sp. OX1. The observation in these latter systems of a diiron(III) oxygenated intermediate having different Mössbauer parameters from analogous species in other carboxylate-bridged diiron proteins is discussed. The results indicate that the ability of the protein framework to tune the reactivity of the diiron center at structurally similar active sites is substantially more complex than previously recognized.

**Introduction**

The biological activation of small substrates, such as dioxygen and dinitrogen, is carried out by large proteins comprising multiple subunits and containing metal cofactors. Examples of these enzymes include nitrogenase, cytochromes P450, tyrosinase, hydrogenase, cytochrome *c* oxidase, and the non-heme carboxylate-bridged diiron proteins. Members of the last family, which include the BMMs, RNR-R2, and  $\Delta^9$ D, activate dioxygen at structurally homologous diiron centers housed within a four-helix bundle. The metal atoms in this bundle are coordinated by the side chains of two E(D/H)XXH motifs.<sup>1</sup> The BMMs exquisitely couple the consumption of electrons and protons to dioxygen activation and substrate hydroxylation. Understanding the management of four substrates

(electrons, protons, dioxygen, and hydrocarbons) in these enzyme systems is a central goal of our research.

In the carboxylate-bridged diiron systems studied thus far, the resting state of the enzyme, which is unreactive toward dioxygen, is a diiron(III) cluster with bridging oxo or hydroxo ligands. Catalysis is initiated by two-electron reduction of this form to generate the reactive diiron(II) state. In systems where crystal structures of the diiron(III) and diiron(II) enzymes, or analogues thereof, are available, reduction is often accompanied by shifting of a dangling, or non-bonded, oxygen atom of a terminal carboxylate ligand to a position bridging the metal ions. The hydroxo or oxo bridges are lost in the process, presumably as water following their protonation.<sup>1,2</sup> The resulting diiron(II) form rapidly reacts with dioxygen to form a peroxodiiron(III) intermediate, which has been characterized by a number of spectroscopic methods (Table 1).<sup>1</sup> In MMO and RNR-R2, this intermediate evolves to higher-valent species Q and X, respectively, which carry out methane hydroxylation or the one-electron oxidation of aromatic amino acid residues (Figure 1). In MMOH, both the peroxodiiron(III) ( $H_{\text{peroxo}}$ ) and Q intermediates are reactive toward substrates,<sup>3</sup> similar to the reactivity observed for oxygenated intermediates in the cytochrome P450 family and some dicopper systems.<sup>4</sup> Part of our ongoing research program has been to develop a more detailed picture of the differential reactivity of the  $H_{\text{peroxo}}$  and Q intermediates in MMOH. The catalytic cycle is closed as the oxygenated intermediates return to the resting diiron(III) state following substrate hydroxylation.

In the present Account, we describe the most recent results on the BMMs MMO, ToMO, and PH. Our discussion begins with a description of the protein components and their interactions. We then proceed through the stages of the catalytic cycle, examining first the ET events, followed by dioxygen activation and, finally, substrate hydroxylation.

**BMM Protein Components**

The BMMs are subdivided into different families, but all contain at least three components in the enzymatic system, a hydroxylase, an NADH oxidoreductase, and a regulatory protein. A fourth, Rieske protein, is also utilized in toluene/alkene monooxygenases.<sup>5</sup> In MMO, ToMO, and PH, the hydroxylase is a dimer of three polypeptide chains,  $(\alpha\beta\gamma)_2$ , with each  $\alpha$ -subunit housing the carboxylate-bridged diiron center, the site of substrate hydroxylation. The oxidoreductase component shuttles electrons from NADH through its bound FAD and  $[2Fe-2S]$  cofactors to the hydroxylase either directly, as in MMO and PH, or indirectly via the Rieske component. The cofactor-less regulatory proteins bind to the hydroxylase and couple electron consumption to hydrocarbon oxidation.<sup>6–8</sup> The

Leslie J. Murray received a B.A. in both chemistry and biology from Swarthmore College in 2002, where he pursued research in synthetic methodology and resonance Raman spectroscopy. He is currently conducting his graduate research at MIT under the supervision of Stephen J. Lippard, investigating dioxygen activation and electron transfer in bacterial multicomponent monooxygenase systems.

Stephen J. Lippard is the Arthur Amos Noyes Professor of Chemistry at MIT. His current research addresses several areas of bioinorganic chemistry including bacterial multicomponent monooxygenases, platinum anticancer drugs, and the detection and functions of biological nitric oxide and mobile zinc(II).

**Table 1. Spectroscopic Parameters for Peroxodiiron(III) Intermediates at Non-heme Diiron Centers**

	Optical <sup>a</sup>		Mössbauer <sup>a</sup>	
	$\lambda_{\text{max}}$ (nm)	$\epsilon$ (M <sup>-1</sup> cm <sup>-1</sup> )	$\delta$ (mm/s)	$\Delta E_Q$ (mm/s)
MMO ( <i>M. caps.</i> )	700	1800	0.66	1.51
MMO ( <i>M. trich.</i> )	725	2500	0.67	1.51
RNR-R2 D84E	700	1500	0.63	1.58
RNR-R2 D84E/W48F	700			
stearoyl-ACP $\Delta^9$ -desaturase	700	1200	0.68	1.90
frog M ferritin	700		0.64	1.06
<i>cis</i> - $\mu$ -1,2-peroxo Fe <sub>2</sub> <sup>III</sup>	650		0.62	1.08
<i>ToMO</i> ( <i>Pseudomonas sporium</i> OX1) <sup>b</sup>	694	2650	0.66	1.40
			0.54	0.67

<sup>a</sup> All parameters except those for ToMO are taken from ref 1. <sup>b</sup> Reference 23.

precise mechanistic consequences of these protein–protein interactions on ET and dioxygen activation are the subject of ongoing research. Very recently, the structure of PHH complexed to its regulatory protein, PHM, was solved, providing the first detailed picture of such an interaction.<sup>9</sup>

## Component Interactions

The assembly of protein complexes during the catalytic cycle must be finely orchestrated to ensure that electron consumption is linked to substrate hydroxylation. For example, reactive oxygenated diiron intermediates in the hydroxylase must not undergo adventitious reduction by the reductase/Rieske protein components.<sup>5</sup> The regulatory protein is proposed to compete with the reductase for a shared binding site on the hydroxylase,<sup>7</sup> thereby protecting oxygenated intermediates formed at the diiron center from undesired reductive quenching following dioxygen activation.<sup>9</sup> On the other hand, ET from these reducing components to the resting, diiron(III) state of the hydroxylase must occur to initiate catalysis. In this section, we discuss studies of the structures and interactions between the regulatory proteins and their respective

hydroxylases and then turn our attention to the ternary system comprising the regulatory, hydroxylase, and reductase/Rieske components.

Crystal structures of BMM hydroxylases from MMO, ToMO, and PH have been solved to date. Three structurally conserved features of note are hydrocarbon access routes, a likely ET pathway to the diiron core, and a pore through the four-helix bundle housing the diiron center for possible dioxygen or proton translocation. Soaking or pressurizing crystals of these proteins with substrate or product analogues has revealed the first of the three shared features, a potential pathway for the entrance or egress of hydrocarbon substrates or products. Soaking ToMOH crystals with the product analogue *p*-bromophenol revealed a large channel that delineates an access pathway from the exterior of the protein through the  $\alpha$ -subunit to the active site (Figure 2).<sup>10</sup> When MMOH crystals were treated with xenon, bromomethanes, or iodoethane, these small hydrophobic species were de-

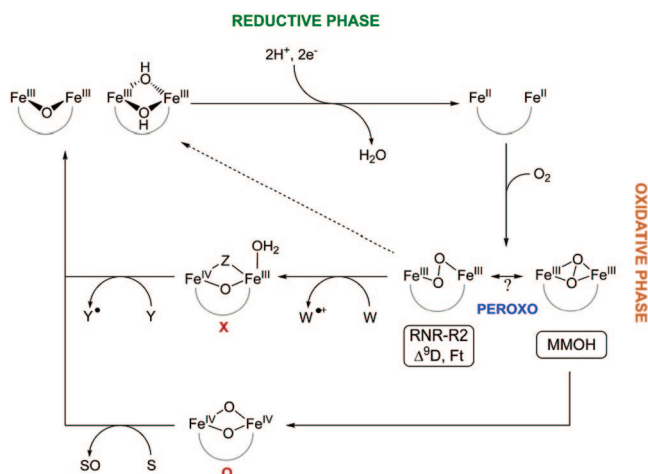


**FIGURE 1.** Dioxygen activation at non-heme carboxylate-bridged diiron centers. Reaction of the reduced diiron(II) state with dioxygen affords a peroxide-bridged intermediate, which can evolve to a high-valent species or decay to the resting diiron(III) state. In MMOH, intermediate Q can oxidize substrates, denoted as S, or decay via other pathways to the resting state. The peroxo intermediate in RNR-R2 oxidizes Trp48 to form X, which then oxidizes Tyr122 to restore the resting diiron(III) state.

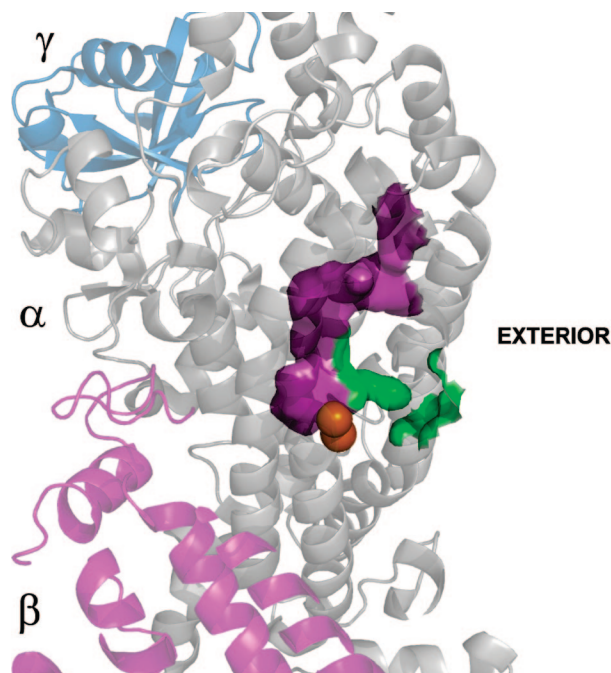


**FIGURE 2.** Substrate access channel and the conserved pore in ToMOH. The access channel (magenta) delineates a path from the diiron center (orange atoms) to the protein surface through the  $\alpha$ -subunit (grey). The conserved pore (green), which is gated by Asn202, extends from the active site pocket to the protein surface. One half of the dimer is depicted.

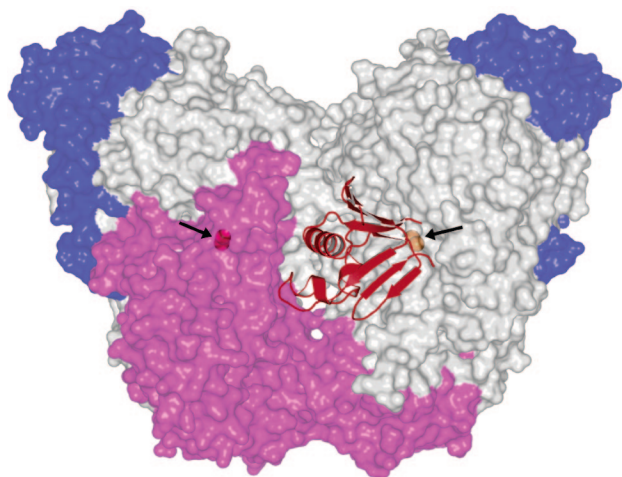


**FIGURE 3.** Crystal structure of PHH in complex with PHM shows the binding of the regulatory protein in the canyon region. The surface of PHH is rendered translucent with the  $\alpha$ -,  $\beta$ -, and  $\gamma$ -subunits depicted in grey, purple, and blue, respectively. The iron atoms are depicted as orange spheres and denoted by arrows. PHM (red) binds to the  $\alpha$ -subunit in a location similar to that predicted for binding of other regulatory proteins to their hydroxylases.

tected in a series of adjacent hydrophobic pockets within the protein that trace a pathway from the protein surface to the diiron center.<sup>11</sup> The distinct pockets are capable of forming a contiguous pathway, as evidenced by structures of crystals soaked with  $\omega$ -halogenated primary alcohols. In these structures, several residues, including Leu110 and Leu289, shift to allow the substrate analogues to traverse the protein cavities.<sup>12</sup> The structure of MMOH crystals soaked with 6-bromohexan-1-ol revealed another property of note. Residues 212–216 in helix E of the  $\alpha$ -subunit unwind to extend the  $\pi$ -character of this helix, reorienting Thr213 and Asn214, residues strictly conserved among the BMMs. The structure of PHH complexed to PHM contains a similarly extended  $\pi$ -helix, providing strong evidence that the binding of regulatory proteins to their respective hydroxylases gives rise to specific conformational changes in helix E that affect the configuration of the active site pocket.<sup>9</sup> The environment around the diiron cluster had been predicted from XAS studies of ToMOH and MMOH in complex with their regulatory proteins<sup>13</sup> to undergo conformational changes, and the PHH–PHM structure provides the first evidence for the nature of these changes.

PHM binds in the canyon region of PHH, specifically on helices E and F, and covers a hydrogen-bonding network from the exterior to the iron-coordinated histidine residues. This feature is the second one conserved among the BMMs (Figures 3 and 4). The locus on PHH where PHM binds, and the predominantly hydrophobic contacts between the proteins, agrees with the predictions of early NMR line-broadening studies carried out on MMOB and MMOH from *M. caps.*<sup>14</sup> The binding site of regulatory proteins in the BMMs may be conserved throughout the family. The hydrogen-bonding network that is covered by PHM, and presumably MMOB, is spatially homologous to the proposed ET pathway in other non-heme diiron proteins.<sup>10</sup> Binding of BMM regulatory

proteins to this surface would interfere with ET for the reasons described above.<sup>5</sup>

The third structurally conserved feature among BMMs is a small pore through the four-helix bundle, which is proximal to the proposed ET pathway and extends from the active site pocket to the protein surface. In most of the crystal structures of BMM hydroxylases, this pore is closed, with a strictly conserved asparagine residue (214, 202, and 204 in MMOH, ToMOH, and PHH, respectively) serving as a gate to the opening. Crystallographic studies reveal this asparagine residue to shift in a redox-dependent manner. Its side chain is oriented away from the active site in the oxidized form and points inward in the reduced or Mn(II) reconstituted forms of the hydroxylase. This motion correlates with the carboxylate shift that occurs upon reduction of the dimetallic center (Figure 5).<sup>1,2</sup> Computational studies predict that dioxygen activation at the diiron(II) core of MMOH is accompanied by dissociation of this carboxylate group from its bridging position.<sup>15</sup> The asparagine gate is open, and the pore provides direct access to the diiron center due to the increased  $\pi$ -character of helix E in the bromohexanol-soaked structure of MMOH.<sup>12</sup> In the  $\alpha$ -subunits of PHH, helix E adopts  $\pi$ -character similar to that in the MMOH bromohexanol-soaked structure, orients Asn204 away from the active site, and opens the pore.<sup>9</sup> PHM is bound only to one face of the PHH dimer and restricts access through this pore for the  $\alpha$ -subunit to which it is bound, but for the other, the pore allows access to the diiron center (Figure 6). The opening of the pore by the shift in Asn204 on the face opposite that to which PHM binds may be an allosteric effect transmitted through the protein dimer interface, arise from interactions with the N-terminus of the  $\beta$ -subunit of the adjacent monomer, or be a consequence of crystal packing. Residue Asn204 in PHH interacts with the hydroxyl side chain of a serine residue of the regulatory protein (Figure 4), suggesting that mechanical strain created when the latter binds to the hydroxylase could promote rearrangement of the shifting carboxylate.<sup>9</sup> The hypothesis<sup>16</sup> that the regulatory protein binds to the hydroxylase and provides a sieve for methane access to the active site at that position is inconsistent with the PHH–PHM structure, and with the observation of CH<sub>2</sub>Br<sub>2</sub>, Xe, and other methane substrate analogues bound in the hydrophobic cavities of MMOH during structure determinations of crystals exposed to these agents. Finally, we note the possibility that dioxygen or protons may enter the active site via the pore.

Among the BMMs, component interactions in MMO isolated either from *M. caps.* or *M. trich.* have been the most extensively studied. Similar interactions were proposed for the binding of MMOB and MMOR to MMOH from studies using chemically modified MMOH.<sup>17</sup> Both MMOR and MMOB bind to MMOH with a 2:1 stoichiometry in the *M. caps.* system, with MMOR binding being an order of magnitude stronger to MMOH than MMOB.<sup>7</sup> In *M. trich.*, MMOB binds 30-fold more weakly to reduced versus oxidized MMOH.<sup>16</sup> The  $K_d$  values determined from the formation and dissociation rate constants of these



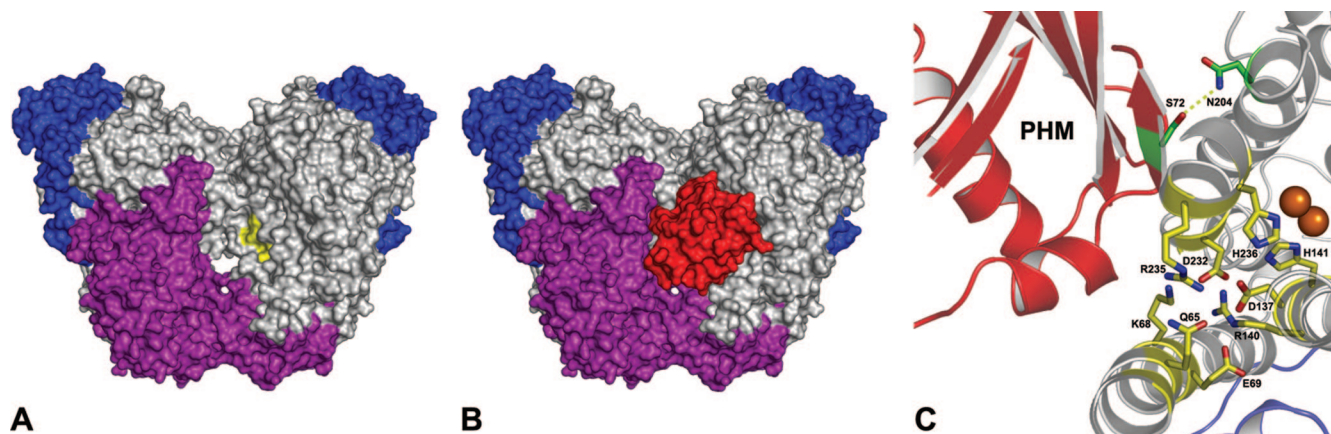


**FIGURE 4.** PHM binds to PHH at the proposed ET pathway and interacts with Asn204. (A) The surface-exposed residues, Arg235 and Lys68, of the conserved hydrogen-bonding network in the  $\alpha$ -subunit are highlighted in yellow on a surface-rendered diagram of PHH. The  $\alpha$ -,  $\beta$ -, and  $\gamma$ -subunits are depicted in grey, purple, and blue, respectively. (B) Diagram A with PHM (red) included. PHM covers this network when complexed to PHH and may prevent the reductase from binding at this locus. (C) A cutaway view, perpendicular to that in A and B, shows that this network, which extends from the iron atoms (orange spheres) to the surface, lies at the interface between the two proteins. PHM also interacts with Asn204 (green sticks), the side chain of which is oriented away from the diiron center as in the oxidized form of the hydroxylase and forms a hydrogen bond with Ser72 of the latter.

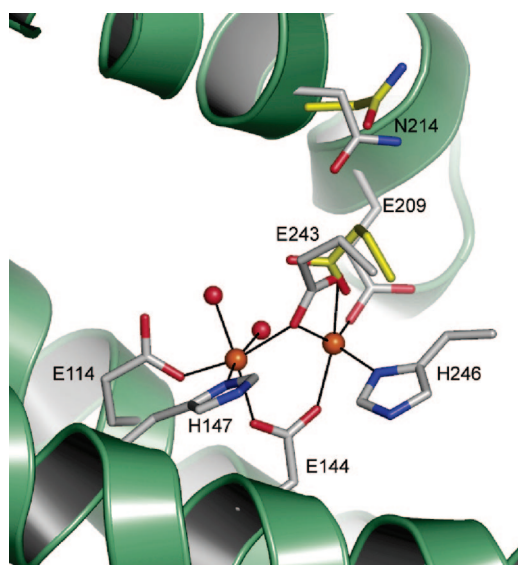


**FIGURE 5.** Redox-state-dependent conformations of residues in the active site pocket of MMOH. The amino acid residues depicted in gray correspond to the reduced state. Residues Glu243 and Asn214 shift upon oxidation (yellow) with Glu243 changing its coordination mode to the dimetallic center.

complexes disagree with the thermodynamic ones, indicative of rapid pre-equilibrium complex formation followed by a slower structural change,<sup>7,16</sup> such as an allosteric effect being transmitted to the other binding site on the dimer. Component binding to one face of the hydroxylase could effect a structural change in the canyon region on the opposite half of the dimer, as noted previously in the PHH–PHM structure. In agreement with the stoichiometry mentioned above, a ratio of 2 MMOB:1 MMOH affords maximal activity for steady-state hydroxylation in the *M. caps.* system. Moreover, enzymatic inhibition occurs at higher ratios of MMOB, suggesting that MMOB saturates the binding sites on MMOH, inhibiting the association of MMOR with MMOH.

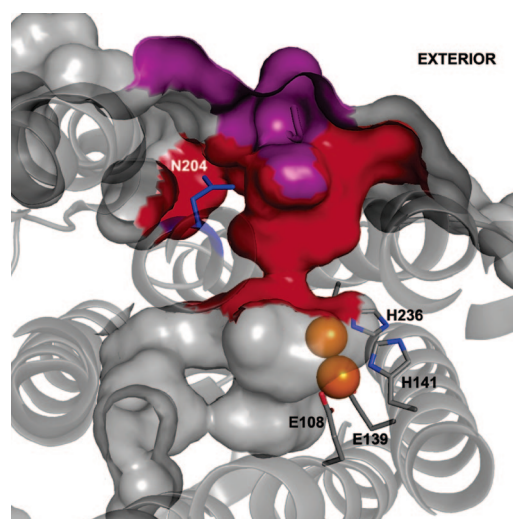


**FIGURE 6.** A surface-rendered representation of the pore in the  $\alpha$ -subunit of PHH to which PHM is *not* bound. Asn204 (blue) is oriented away from the diiron center, opens the pore (red), and allows access from the protein exterior to the diiron center (orange spheres). Four iron-binding ligands, Glu108, Glu139, His236, and His141, are identified. This structural change may arise from PHM binding at the opposing face, interactions with the N-terminus of the  $\beta$ -subunit from the opposing monomer (purple), or packing in the crystal.

## Electron Transfer to the Oxidized Hydroxylase

An early study of ET from NADH to the diiron(III) centers in oxidized MMOH, premixed with MMOR and variable equivalents of MMOB, demonstrated that all but one of the ET events are enhanced by MMOB.<sup>7</sup> More recently, an investigation of the reaction of chemically reduced MMOR or MMOR-Fd with MMOH–MMOB mixtures showed the opposite effect, in which MMOB served to *inhibit* ET.<sup>18</sup> These two apparently contradictory effects of MMOB on ET may be a consequence of a slow structural change associated with MMOB or MMOR binding to MMOH.<sup>18</sup> The conclusion that hysteresis may

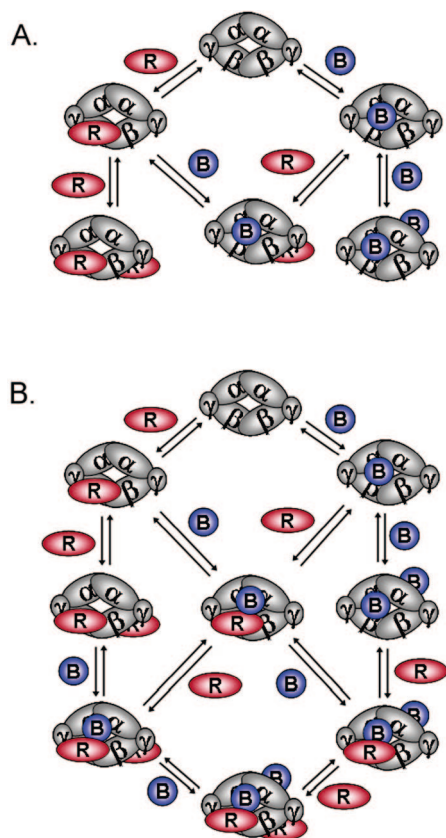


**FIGURE 7.** Component interactions in the BMMs depicting a half-sites mechanism (A) and a non-interacting sites model (B). In diagram A, one active site is undergoing reduction while the second is activating dioxygen. In diagram B, a ternary complex may form but is not obligatory for catalysis and may have implications for ET and dioxygen activation. The regulatory component is depicted as B, and the reductase (MMO and PH) or Rieske (ToMO) component as R. Adapted from ref 7.

control the activity of MMOH was similarly drawn from an analysis of the product distributions when various substrates were hydroxylated by MMO from *M. trich*.<sup>19</sup> The interaction of MMOH with either MMOR or MMOB may depend on the presence or absence of the other component. The two may bind either concurrently, on opposing canyon regions of MMOH, or in rapid succession at the same canyon region on one side of the hydroxylase.

These two scenarios for the interaction of the components during the catalytic cycle are illustrated in Figure 7. In the half-sites reactivity mechanism, the reductase binds on one canyon surface for ET while the regulatory protein binds on the other canyon surface for dioxygen activation and substrate hydroxylation (Figure 7A). Hysteresis would reflect binding of the regulatory and the reductase components to the opposite faces of the hydroxylase, thereby predisposing each diiron center to traverse opposite segments of the catalytic cycle. RFQ Mössbauer experiments performed to investigate the reaction of reduced MMOH,<sup>20</sup> PHH,<sup>21</sup> and ToMOH<sup>22</sup> with dioxygen consistently have recorded a maximal conversion of ~50% of the initial diiron(II) protein to the oxygenated intermediates. This result suggests that the oxidative phase of the catalytic cycle can occur only at

one active site of the dimer, irrespective of whether both active sites are fully reduced. Half-sites reactivity has also been proposed in other non-heme diiron proteins, in particular  $\Delta^9\text{D}^{23}$  and RNR-R2,<sup>24</sup> and may be a conserved feature in these systems. A different scenario, depicted in Figure 7B, is that the regulatory protein binds loosely to the hydroxylase and is displaced partially or shifts in the presence of the reductase to form a ternary complex that is competent for ET and catalysis. Further work is necessary to acquire a more complete understanding of the nature of these component interactions and their role in catalysis.

## Formation and Reactivity of Activated Dioxygen Intermediates

**Steady State Studies.** The mechanism of hydrocarbon hydroxylation by the BMMs under steady state conditions has been examined primarily with radical clock substrate (RCS) probes. These hydrocarbons often contain strained rings that open with a characteristic lifetime following the loss of a hydrogen atom. Radical-derived ring-opened products will be observed only if their recombination rate is slower than ring expansion, in which case the lifetime of the radical can be estimated from ratios of the rearranged to unrearranged product alcohols. In general, only unrearranged products arising from rapid recombination of bound radical species are observed for most of the RCS probes tested in MMO, and their lifetime has been estimated to be <150 fs.<sup>1,25</sup> In addition to ring expansion from H-atom abstraction from the substrate, some RCS probes can ring-open following hydride abstraction to yield products that differ from the radical-derived ones. Norcarane, methylcubane, and 1,1-dimethylcyclopropane are examples of such RCS probes, and the major products formed in steady state catalysis by ToMO,<sup>26</sup> T4MO,<sup>27</sup> and MMO<sup>1</sup> with these substrates are the unrearranged alcohols. Little or no rearranged products, either radical- or carbocation-derived, are observed for these substrates in reactions with T4MO and MMO, in agreement with the other RCS experiments mentioned above. For the oxidation of norcarane by MMO, ring-expansion products from both intermediates formed and the product ratios placed a lower limit of 20 ps on the radical lifetime, significantly greater than the value determined from any other probe. Oxidation of this RCS by T4MO afforded a radical-rearranged product (4.5% of the total), and no carbocation-derived product could be detected, contrary to the results from the oxidation of both 1,1-dimethyl- and 1,1-diethylcyclopropane.<sup>27</sup> A recent reexamination of the norcarane reaction for MMO and ToMO revealed that desaturation of the substrate by BMMs can explain these discrepancies.<sup>26</sup> Evidence for both a hydride and an H-atom transfer mechanism suggests that more than one reactive oxygenated intermediate may be involved.

**Transient Kinetic Studies.** In the oxidative phase of the catalytic cycle (Figure 1), the regulatory protein is required for the formation of detectable intermediates<sup>28</sup> and tunes the regioselectivity of substrate hydroxylation.<sup>29</sup>



Transient, pre-steady state kinetic studies have been performed with chemically reduced mixtures of the hydroxylases and their regulatory proteins to study the reactivity of individual intermediates during the reaction of dioxygen with the reduced BMM hydroxylases. In particular, we have utilized single- and double-mixing stopped-flow methodologies in such investigations whereby a solution of reduced hydroxylase with its regulatory protein is mixed rapidly with dioxygen and allowed to age for a time period that maximizes the formation of an intermediate of interest, and the aged solution is subsequently mixed with buffer containing substrate. Loss of an optical absorption band characteristic of the intermediate,<sup>3</sup> or of an infrared band of a substrate,<sup>30</sup> is measured as a function of substrate concentration. Among the BMMs, this strategy has been the most effective for investigating the reactions of MMOH with dioxygen since both H<sub>peroxo</sub> and Q have characteristic absorption bands. The effect of substrates on the decay rate of each intermediate can be readily monitored by recording a change in these optical features. Initial studies of MMO in which propylene, methane, and acetylene were used as substrates indicated that H<sub>peroxo</sub> reacts only with propylene whereas Q reacts with all three substrates.<sup>3</sup> Previous steady-state studies revealed that terminal alkenes are epoxidized by MMO with no C–H bond activation.<sup>31</sup> Although Q oxidizes propylene faster than H<sub>peroxo</sub>, a judiciously chosen substrate might react more rapidly with H<sub>peroxo</sub> than Q to confirm that H<sub>peroxo</sub> is a reactive species. We extended our work to include ethyl vinyl ether and diethyl ether and discovered that both of these substrates react more rapidly with H<sub>peroxo</sub> than with Q.<sup>4</sup> From a detailed investigation of the oxidation of these substrates, it appears that H<sub>peroxo</sub> is a more electrophilic oxidant than Q, preferring to react by a two-electron, or a hydride abstraction, pathway, whereas one-electron oxidation processes are preferred by Q (Figure 8). This difference in reactivity may explain the carbocation-derived products in the RCS probe experiments because reaction of H<sub>peroxo</sub> with these substrates could form transient carbocations.

In contrast to what we observe for H<sub>peroxo</sub>, peroxodiiiron(III) intermediates in ferritin, mutants of RNR-R2, Δ<sup>9</sup>D, and model compounds have no observed reactivity towards hydrocarbons. These species have been characterized by rR spectroscopy, from which it appears that the peroxide moiety bridges the dimetallic center in a  $\mu$ -1,2 fashion. Although a rR spectrum has not yet been obtained for H<sub>peroxo</sub>, computational methods predict that a  $\mu$ - $\eta^2$ : $\eta^2$ -peroxo butterfly structure is more stable than the alternative  $\mu$ -1,2 geometry of the bound peroxide.<sup>32</sup> The occurrence of such a binding mode in H<sub>peroxo</sub> may explain why it reacts with electron-rich hydrocarbons and why a Q-type species is *only* observed in MMO. The difference in reactivity between H<sub>peroxo</sub> and Q parallels the known differences between ( $\mu$ - $\eta^2$ : $\eta^2$ -peroxo)dicopper(II) species, which react by two-electron processes, and high-valent di( $\mu$ -oxo)dicopper(III) centers, which prefer sequential one-electron oxidations, in the dicopper complexes. From

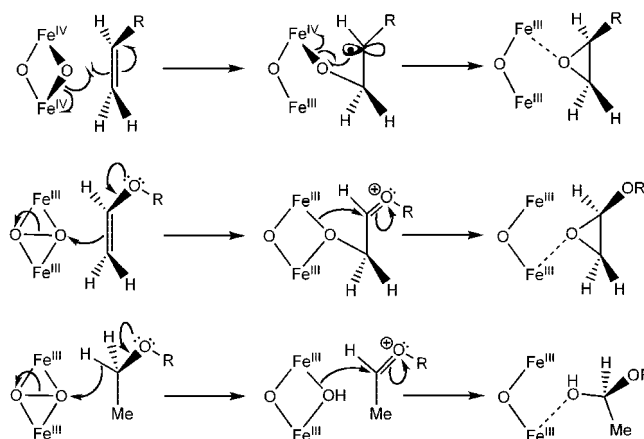


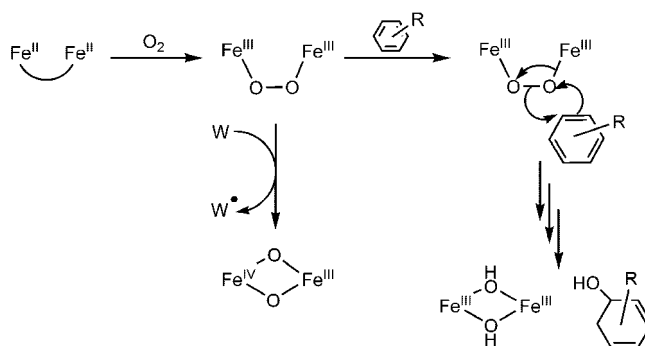
**FIGURE 8.** Proposed mechanism for reaction of Q and H<sub>peroxo</sub> with substrates. Q reacts by sequential one-electron oxidations (upper). Reaction of H<sub>peroxo</sub> with ethyl vinyl ether proceeds by a two-electron mechanism, in which a transient carbocation is stabilized by the proximal oxygen atom (middle). Hydroxylation of diethyl ether by H<sub>peroxo</sub> is also proposed to proceed by a two-electron process, in which hydride abstraction forms a transient carbocation that recombines with the coordinated hydroxide (lower). Adapted from ref 4.

theoretical studies on MMOH, compression of the diiron cluster by the protein scaffold at the active site favors formation of a ( $\mu$ - $\eta^2$ : $\eta^2$ -peroxo)diiiron(III) structure and its subsequent conversion to Q.<sup>32</sup> It will be interesting to learn whether such an effect may be absent in other BMM hydroxylases, where the peroxo spectral parameters differ and a diiron(IV) species has not yet been observed.

Until recently, no intermediates were reported during stopped-flow optical spectroscopic study of the reactions of reduced ToMOH or PHH, complexed with their respective regulatory proteins, with O<sub>2</sub>-saturated buffer. Comparison of the crystal structures of ToMOH and MMOH reveal that Ile100 in the former is analogous to a leucine residue in the latter that is proposed to gate substrate access to the diiron site during catalysis.<sup>33</sup> We therefore prepared an I100W mutant in the  $\alpha$ -subunit of ToMOH with the aim of retarding access of any buffer components to the diiron site that might quench high-valent intermediates before they could build up to an observable level.<sup>10,33</sup> The reaction of the reduced ToMOH I100W mutant and ToMOD with dioxygen was studied by stopped-flow optical spectroscopy and by RFQ EPR and Mössbauer spectroscopy. These methods revealed intermediates in the ToMO system for the first time. One of the species contains a mixed-valent diiron(III,IV) cluster coupled to a tryptophanyl radical involving the mutated residue.<sup>22</sup> The other, a diiron(III) intermediate, was subsequently also encountered in experiments on the wild-type hydroxylase.<sup>34</sup>

The transient, neutral tryptophanyl radical that forms during oxygenation of the I100W ToMOH mutant has an absorption maximum at 500 nm and an EPR signal at  $g \approx 2.0$ , which forms and decays with rate constants similar to those encountered in the optical studies. This EPR spectrum is comparable to that of the X-W<sup>•+</sup> couple in the RNR-R2 D84E mutant.<sup>22</sup> To determine whether the

Scheme 1



reaction of the ToMOH mutant with dioxygen proceeds by the same mechanism as that proposed for RNR-R2, which involves either a peroxodiiron(III) or a short-lived di( $\mu$ -oxo)diiron(IV) center that is postulated to abstract an electron from a nearby residue, we investigated the diiron center during the course of the reaction by RFQ Mössbauer spectroscopy. The results confirmed that, in the ToMOH mutant, the neutral tryptophanyl radical is coupled to a mixed-valent diiron(III,IV) cluster, the Mössbauer spectrum of which is well-modeled by the same parameters used to fit the X-W<sup>•+</sup> species in the aforementioned RNR-R2 mutant.

Mössbauer spectra at reaction times preceding the formation of the X-analogue in the ToMOH I100W mutant display a quadrupole doublet that forms rapidly upon the mixing of ToMOH<sub>red</sub> complexed with ToMOD and dioxygen and that could be kinetically linked to formation of the mixed-valent diiron(III,IV) species. The early diiron(III) intermediate is diamagnetic, as evidenced by the lack of an EPR signal and indifference of the Mössbauer spectrum to an applied magnetic field in the RFQ samples.<sup>34</sup> Thus, an intermediate having no distinctive optical absorption bands forms during oxidation of the reduced I100W mutant and evolves to a mixed-valent center, possibly by one-electron abstraction from Trp100.

Investigation of the oxygenation of reduced native hydroxylase by RFQ Mössbauer spectroscopy revealed the same diiron(III) intermediate with isomer shift,  $\delta$ , and quadrupole splitting,  $\Delta E_Q$ , parameters similar to those for the I100W diiron(III) transient.<sup>34</sup> This intermediate is longer-lived than that in the I100W mutant, presumably because it lacks a nearby redox-active residue. From double-mixing RFQ Mössbauer spectroscopy, we determined that phenol, a substrate in this system, induces the diiron(III) intermediate to decay to the diiron(III) resting state of ToMOH more rapidly than in its absence. No additional diiron intermediates were observed. In single-turnover experiments, phenol is oxidized exclusively to catechol, implying that the diiron(III) transient is kinetically competent, catalytically relevant, and possibly the key active oxidant in the system.

The Mössbauer  $\delta$  and  $\Delta E_Q$  parameters for the oxygenated ToMOH intermediate and the absence of distinguishable visible or near-IR optical absorbance bands are noteworthy differences from peroxodiiron(III) clusters characterized in carboxylate-bridged diiron proteins and model complexes (Table 1). We tentatively assign this novel species as a peroxodiiron(III) center, where the peroxide moiety has a different binding mode or protonation state from those previously observed, although we have no direct evidence for the presence of an O<sub>2</sub><sup>2-</sup> unit. A diiron(III) intermediate with very similar Mössbauer parameters has recently been observed in the native PHH isolated from the same organism.<sup>21</sup>

The foregoing mechanism for dioxygen activation in ToMO parallels the related processes in MMO and RNR-R2. The diiron(II) state reacts with dioxygen to afford a

peroxodiiron(III) intermediate, which can be an active oxidant. This transient reacts with aromatic substrates or abstracts an electron from the nearby W (Scheme 1). Protein matrix effects and/or regulatory component interactions may trigger the peroxodiiron(III) intermediate to evolve into the high-valent intermediate Q in MMO. An analogous mechanism is proposed for RNR-R2, where a peroxo-bridged transient or a short-lived diiron(IV) intermediate abstracts an electron from nearby redox active residues in the native system<sup>5</sup> or hydroxylates a nearby phenylalanine in the D84E/Y122F double mutant.<sup>35</sup> If such a diiron(IV) transient forms in ToMOH, it must be short-lived since RFQ Mössbauer samples do not indicate the occurrence of such a species. The inability of ToMO and PH to hydroxylate methane under steady state conditions suggests that Q-type intermediates do not arise in these systems. Furthermore, NIH shift experiments on the related T4MO system reveal that a transient arene epoxide or cationic substrate intermediate is formed,<sup>36</sup> reminiscent of the two-electron oxidations of unsaturated substrates by H<sub>peroxo</sub> and not the one-electron oxidations afforded by Q.

## Summary and Outlook

Oxygenated diiron intermediates and the nature and effects of protein–protein interactions have been studied in the BMM family. H<sub>peroxo</sub> and Q in MMOH have demonstrated reactivity toward substrates, oxidizing them by different mechanisms. Recent investigations of ToMOH and PHH have revealed the presence of kinetically competent, oxygenated diiron(III) intermediates, spectroscopically different from previously reported oxygenated diiron(III) intermediates at other carboxylate-bridged diiron centers, highlighting the ability of the four-helix bundle motif and possibly the surrounding protein matrix to determine the active species involved in catalysis. The chemical and structural consequences of component interactions on dioxygen activation and ET were investigated by transient, steady state, and crystallographic methods, and the last approach has afforded the first definitive structural information about any hydroxylase–regulatory protein complex in these systems. Many important questions still remain for the BMM family of enzymes, however. The pathways by which electrons and protons access the diiron cores during reduction is still

an open question, although a conserved hydrogen bonding network is suggested to be the ET pathway by comparison to other carboxylate-bridged diiron proteins. A definitive structural assignment of the oxygenated intermediates in the BMMs is essential for a mechanistic understanding of dioxygen activation in these systems. The structural and chemical effects of protein complexes, which are important for catalysis, on ET or proton translocation, dioxygen activation, and substrate hydroxylation are incompletely understood. Ongoing research is focused on understanding these components of the catalytic cycle and their role in modulating the reactivity of these similar diiron cores.

## Abbreviations

BMM, bacterial multicomponent monooxygenase;  $\Delta^9$ D, stearoyl-ACP  $\Delta^9$  desaturase; EPR, electron paramagnetic resonance; ET, electron transfer; FAD, flavin adenine dinucleotide; H<sub>peroxo</sub>, peroxodiiron(III) intermediate in MMOH; *M. caps.*, *Methylococcus capsulatus* (Bath); *M. trich.*, *Methylosinus trichosporium* OB3b; MMO, soluble methane monooxygenase; MMOB, regulatory protein in MMO; MMOH, hydroxylase component of MMO; MMOR, NADH oxidoreductase component of MMO; MMOR-Fd, truncated MMOR containing only the ferredoxin domain; NADH, reduced nicotinamide adenine dinucleotide; PH, phenol hydroxylase; PHH, hydroxylase component of PH; PHM, regulatory protein of PH; RCS, radical-clock substrate; RFQ, rapid-freeze quench; RNR-R2, ribonucleotide reductase R2 subunit (Class 1); rR, resonance Raman; T4MO, toluene 4-monooxygenase; ToMO, toluene/*o*-xylene monooxygenase; ToMOC, Rieske component in ToMO; ToMOD, regulatory protein in ToMO; ToMOH, hydroxylase in ToMO; XAS, X-ray absorption spectroscopy.

Work from our laboratory covered in this Account was supported by the National Institute of General Medical Sciences.

## References

- (1) Merckx, M.; Kopp, D. A.; Sazinsky, M. H.; Blazyk, J. L.; Müller, J.; Lippard, S. J. Dioxygen activation and methane hydroxylation by soluble methane monooxygenase: A tale of two irons and three proteins. *Angew. Chem., Int. Ed.* **2001**, *40*, 2782–2807 and references cited therein.
- (2) McCormick, M. S.; Sazinsky, M. H.; Condon, K. L.; Lippard, S. J. X-ray crystal structures of manganese(II)-reconstituted and native toluene/*o*-xylene monooxygenase hydroxylase reveal rotamer shifts in conserved residues and an enhanced view of the protein interior. *J. Am. Chem. Soc.* **2006**, *128*, 15108–15110.
- (3) Valentine, A. M.; Stahl, S. S.; Lippard, S. J. Mechanistic studies of the reaction of reduced methane monooxygenase hydroxylase with dioxygen and substrates. *J. Am. Chem. Soc.* **1999**, *121*, 3876–3887.
- (4) Beauvais, L. G.; Lippard, S. J. Reactions of the peroxo intermediate of soluble methane monooxygenase with ethers. *J. Am. Chem. Soc.* **2005**, *127*, 7370–7378 and references cited therein.
- (5) Sazinsky, M. H.; Lippard, S. J. Correlating structure with function in bacterial multicomponent monooxygenases and related diiron proteins. *Acc. Chem. Res.* **2006**, *39*, 558–566 and references cited therein.
- (6) Fox, B. G.; Liu, Y.; Dege, J. E.; Lipscomb, J. D. Complex formation between the protein components of methane monooxygenase from *Methylosinus trichosporium* OB3b: Identification of sites of component interaction. *J. Biol. Chem.* **1991**, *266*, 540–550.
- (7) Gassner, G. T.; Lippard, S. J. Component interactions in the soluble methane monooxygenase system from *Methylococcus capsulatus* (Bath). *Biochemistry* **1999**, *38*, 12768–12785.
- (8) Dalton, H. The natural and unnatural history of methane-oxidizing bacteria. *Philos. Trans. R. Soc. London, Ser. B* **2005**, *360*, 1207–1222.
- (9) Sazinsky, M. H.; Dunten, P. W.; McCormick, M. S.; DiDonato, A.; Lippard, S. J. X-ray structure of a hydroxylase-regulatory protein complex from a hydrocarbon-oxidizing multicomponent monooxygenase, *Pseudomonas* sp. OX1 phenol hydroxylase. *Biochemistry* **2006**, *45*, 15392–15404.
- (10) Sazinsky, M. H.; Bard, J.; DiDonato, A.; Lippard, S. J. Crystal structure of the toluene/*o*-xylene monooxygenase hydroxylase from *Pseudomonas stutzeri* OX1: Insight into the substrate specificity, substrate channeling, and active site tuning of multicomponent monooxygenases. *J. Biol. Chem.* **2004**, *279*, 30600–30610 and references cited therein.
- (11) Whittington, D. A.; Rosenzweig, A. C.; Frederick, C. A.; Lippard, S. J. Xenon and halogenated alkanes track putative substrate binding cavities in the soluble methane monooxygenase hydroxylase. *Biochemistry* **2001**, *40*, 3476–3482.
- (12) Sazinsky, M. H.; Lippard, S. J. Product bound structures of the soluble methane monooxygenase hydroxylase from *Methylococcus capsulatus* (Bath): Protein motion in the  $\alpha$ -subunit. *J. Am. Chem. Soc.* **2005**, *127*, 5814–5825.
- (13) Jackson Rudd, D.; Sazinsky, M. H.; Lippard, S. J.; Hedman, B.; Hodgson, K. O. X-ray absorption spectroscopic study of the reduced hydroxylases of methane monooxygenase and toluene/*o*-xylene monooxygenase: Differences in active structure and effects of the coupling proteins MMOB and ToMOD. *Inorg. Chem.* **2005**, *44*, 4546–4554.
- (14) Walters, K. J.; Gassner, G. T.; Lippard, S. J.; Wagner, G. Structure of the soluble methane monooxygenase regulatory protein B. *Proc. Natl. Acad. Sci. U.S.A.* **1999**, *96*, 7877–7882.
- (15) Gherman, B. F.; Baik, M.-H.; Lippard, S. J.; Friesner, R. A. Dioxygen activation in methane monooxygenase: A theoretical study. *J. Am. Chem. Soc.* **2004**, *126*, 2978–2990.
- (16) Zhang, J.; Wallar, B. J.; Popescu, C. V.; Renner, D. B.; Thomas, D. D.; Lipscomb, J. D. Methane monooxygenase hydroxylase and B component interactions. *Biochemistry* **2006**, *45*, 2913–2926.
- (17) Balendra, S.; Lesieur, C.; Smith, T. J.; Dalton, H. Positively charged amino acids are essential for electron transfer and protein-protein interactions in the soluble methane monooxygenase complex from *Methylococcus capsulatus* (Bath). *Biochemistry* **2002**, *41*, 2571–2579.
- (18) Blazyk, J. L.; Gassner, G. T.; Lippard, S. J. Intermolecular electron-transfer reactions in soluble methane monooxygenase: A role for hysteresis in protein function. *J. Am. Chem. Soc.* **2005**, *127*, 17364–17376.
- (19) Froland, W. A.; Andersson, K. K.; Lee, S.-K.; Liu, Y.; Lipscomb, J. D. Methane monooxygenase component B and reductase alter the regioselectivity of the hydroxylase component-catalyzed reactions: A novel role for protein-protein interactions in an oxygenase mechanism. *J. Biol. Chem.* **1992**, *267*, 17588–17597.
- (20) Liu, K. E.; Valentine, A. M.; Wang, D.; Huynh, B. H.; Edmondson, D. E.; Salifoglou, A.; Lippard, S. J. Kinetic and spectroscopic characterization of intermediates and component interactions in reactions of methane monooxygenase from *Methylococcus capsulatus* (Bath). *J. Am. Chem. Soc.* **1995**, *117*, 10174–10185.
- (21) Izzo, V.; Tinberg, C. E.; García-Serres, R.; Naik, S.; Huynh, B. H.; Lippard, S. J. Unpublished results.
- (22) Murray, L. J.; García-Serres, R.; Naik, S.; Huynh, B. H.; Lippard, S. J. Dioxygen activation at non-heme diiron centers: Characterization of intermediates in a mutant form of toluene/*o*-xylene monooxygenase hydroxylase. *J. Am. Chem. Soc.* **2006**, *128*, 7458–7459.
- (23) Broadwater, J. A.; Ai, J.; Loehr, T. M.; Sanders-Loehr, J.; Fox, B. G. Peroxodiferric intermediate of stearoyl-acyl carrier protein  $\Delta^9$  desaturase: Oxidase reactivity during single turnover and implications for the mechanism of desaturation. *Biochemistry* **1998**, *37*, 14664–14671.
- (24) Sjöberg, B.-M.; Karlsson, M.; Jörnvall, H. Half-site reactivity of the tyrosyl radical of ribonucleotide reductase from *Escherichia coli*. *J. Biol. Chem.* **1987**, *262*, 9736–9743.
- (25) Baik, M.-H.; Newcomb, M.; Friesner, R. A.; Lippard, S. J. Mechanistic studies on the hydroxylation of methane by methane monooxygenase. *Chem. Rev.* **2003**, *103*, 2385–2419.
- (26) Newcomb, M.; Chandrasena, R. E. P.; Lansakara-P., D. S. P.; Kim, H.-Y.; Lippard, S. J.; Beauvais, L. G.; Murray, L. J.; Izzo, V.; Hollenberg, P. F.; Coon, M. J. Desaturase reactions complicate the use of norcarane as a mechanistic probe. Unraveling the mixture of twenty-plus products formed in enzyme-catalyzed oxidations of norcarane. *J. Org. Chem.* **2007**, *72*, 1121–1127.



- (27) Moe, L. A.; Hu, Z.; Deng, D.; Austin, R. N.; Groves, J. T.; Fox, B. G. Remarkable aliphatic hydroxylation by the diiron enzyme toluene 4-monooxygenase in reactions with radical or cation diagnostic probes norcarane, 1,1-dimethylcyclopropane, and 1,1-diethylcyclopropane. *Biochemistry* **2004**, *43*, 15688–15701.
- (28) Liu, Y.; Nesheim, J. C.; Lee, S.-K.; Lipscomb, J. D. Gating effects of component B on oxygen activation by the methane monooxygenase hydroxylase component. *J. Biol. Chem.* **1995**, *270*, 24662–24665.
- (29) Lipscomb, J. D. Biochemistry of the soluble methane monooxygenase. *Annu. Rev. Microbiol.* **1994**, *48*, 371–399.
- (30) Muthusamy, M.; Ambundo, E. A.; George, S. J.; Lippard, S. J.; Thorneley, R. N. F. Stopped-flow fourier transform infrared spectroscopy of nitromethane oxidation by the diiron(IV) intermediate of methane monooxygenase. *J. Am. Chem. Soc.* **2003**, *125*, 11150–11151.
- (31) Colby, J.; Stirling, D. I.; Dalton, H. The soluble methane monooxygenase of *Methylococcus capsulatus* (Bath): Its ability to oxygenate *n*-alkanes, *n*-alkenes, ethers and alicyclic, aromatic and heterocyclic compounds. *Biochem. J.* **1977**, *165*, 395–402.
- (32) Rinaldo, D.; Philipp, D. M.; Lippard, S. J.; Friesner, R. A. Intermediates in dioxygen activation by methane monooxygenase: A QM/MM study. *J. Am. Chem. Soc.* **2007**, *129*, 3135–3147.
- (33) Rosenzweig, A. C.; Brandstetter, H.; Whittington, D. A.; Nordlund, P.; Lippard, S. J.; Frederick, C. A. Crystal structures of the methane monooxygenase hydroxylase from *Methylococcus capsulatus* (Bath): Implications for substrate gating and component interactions. *Proteins* **1997**, *29*, 141–152.
- (34) Murray, L. J.; García-Serres, R.; Naik, S.; Huynh, B. H.; Lippard, S. J., in preparation.
- (35) Baldwin, J.; Voegtli, W. C.; Khidekel, N.; Moënne-Loccoz, P.; Krebs, C.; Pereira, A. S.; Ley, B. A.; Huynh, B. H.; Loehr, T. M.; Riggs-Gelasco, P. J.; Rosenzweig, A. C.; Bollinger, J. M., Jr. Rational reprogramming of the R2 subunit of *Escherichia coli* ribonucleotide reductase into a self-hydroxylating monooxygenase. *J. Am. Chem. Soc.* **2001**, *123*, 7017–7030.
- (36) Mitchell, K. H.; Rogge, C. E.; Gierahn, T.; Fox, B. G. Insight into the mechanism of aromatic hydroxylation by toluene 4-monooxygenase by use of specifically deuterated toluene and *p*-xylene. *Proc. Natl. Acad. Sci. U.S.A.* **2003**, *100*, 3784–3789.

AR600040E